

Theoretical study on the second-order nonlinear optical properties and reorganization energy of silafluorenes and spirobisilafluorenes derivatives

Yanling Si · Guochun Yang

Received: 29 June 2010/Accepted: 14 October 2010/Published online: 3 November 2010
© Springer-Verlag 2010

Abstract The electronic absorption and emission spectra, second-order polarizability and reorganization energy of the twenty silafluorenes and spirobisilafluorenes derivatives have been studied at the density functional theory level. The results show that the second-order polarizability (β) increases with increase in the number of the branches due to cooperative enhancement of the charge transfer, whereas the reorganization energy (λ) follows the opposite trend for the studied compounds. The properties (β and λ) of the compounds at the 3, 6-positions substitution are much better than those of compounds at the 2, 7-positions substitution. The effects of donor/acceptor (D/A) substitution and different spiroatoms (silicon or carbon) on second-order polarizability and reorganization energy are also discussed. It is noted that the charge transport properties can be tuned by changing the donor/acceptor (D/A) substitution, and the acceptor substitution can greatly reduce the reorganization energy. The electronic absorption spectra show that all studied compounds can meet the requirement of nonlinear optical (NLO) transparency. Thus, increasing the number of branches and acceptor substitution can remarkably enhance performance of this

kind of compounds. Based on larger β , smaller λ and excellent optical transparency, this kind of compounds have a possibility to be excellent second-order NLO or charge transport materials.

Keywords Spirobisilafluorenes · Nonlinear optical properties · Charge transport · Electronic spectra · DFT

1 Introduction

Organic molecules have the advantage of easy chemical modifications for structural diversity, easy fabrication, mechanical flexibility, and low cost. Thus, the development of organic molecular and polymeric compounds has brought forth a number of remarkable discoveries in electronic, optoelectronic, and electrooptic devices [1, 2]. The continued emergence of these new technologies will mainly depend on performance enhancement in such matters as nonlinear optical (NLO) response, luminescence quantum efficiency, charge injection and transport efficiency, and temporal and thermal stability.

Materials with large hyperpolarizabilities are good candidates for use in optoelectronics and a variety of optical devices [3–11]. There exist three generic classes of NLO material: semiconductors, inorganic salts, and organic compounds. Each class possesses its own complement of favorable and unfavorable attributes for NLO application [12]. The organic materials are of major interest because of their larger NLO coefficient, high laser damage thresholds, low dielectric constants, fast nonlinear optical response times, and off-resonance nonlinear optical susceptibilities comparable to or exceeding those of ferroelectric inorganic crystals [13]. Organic materials have several disadvantages: low energy transitions in the

Electronic supplementary material The online version of this article (doi:[10.1007/s00214-010-0838-z](https://doi.org/10.1007/s00214-010-0838-z)) contains supplementary material, which is available to authorized users.

Y. Si
College of Resource and Environmental Science,
Jilin Agricultural University, Changchun, Jilin 130118,
People's Republic of China

Y. Si · G. Yang (✉)
Institute of Functional Material Chemistry,
Faculty of Chemistry, Northeast Normal University,
Changchun 130024, People's Republic of China
e-mail: yanggc468@nenu.edu.cn

UV-vis region enhance the NLO efficiency but result in a trade-off between nonlinear efficiency and optical transparency, they may have low thermal stability, and (in poled guest–host systems) they may undergo a facile relaxation to random orientation [14]. Thus, it is very important to find suitable organic materials with larger NLO response, excellent optical transparency and thermal stability.

Organic semiconductors are of interest for manufacturing large-area and flexible organic electronic devices at low cost. The reliability of organic electronic devices depends on the morphological stability of the corresponding materials, which can be quantified by the glass-transition temperature (T_g) of the materials [15]. The efficiency of OLEDs is determined by charge injection and transport, charge carrier balance, radiative decay of excitons, and light extraction. However, charge transport in organic materials is one of the most important properties in the performance of organic light-emitting devices (OLEDs) [16, 17], organic field effect transistors (OFETs) [18, 19], and organic solar cells [20, 21]. Higher carrier mobilities in the charge transport process depend on smaller reorganization energy and larger transfer integral.

The bonding concept of spiroconjugation was introduced some years ago by Hoffmann [22] and simultaneously by Simons and Fukunaga [23]. To the spiroconjugated compounds, significant exchange interaction across the spiroatom can be obtained without being accompanied by the reduction in the excitation energy, which can satisfy optical transparency. Both experimental results [24] and theoretical studies [25–29] show that spiroconjugated compounds exhibit excellent NLO properties and excellent optical transparency. In 1996, a surprisingly variable concept for the design of amorphous electroluminescent materials with high T_g is based on the specific introduction of spiro-center into defined low molecular structures [30]. They used the known structures which already have the desired electronic or optical properties and to modify their steric demand in such a way that their processability and morphologic stability is improved, while their electronic properties are retained [31–33]. Based on Spiro-TAD and Spiro-PDB, they obtained blue electroluminescence devices with high color purity, high brightness, high T_g , and low turn-on voltage [32]. Now, spiro-linked compounds are known to be glass-forming materials with high T_g and good morphological stability, which makes them well-suited for organic devices. Spiro-linked compounds have been successfully applied in OLEDs [34, 35], OFETs [36–38], phototransistors [39, 40], and lasers [41–44].

Recently, Kawashima et al. have synthesized and characterized a series of π -Extended silafluorenes and spirobisilafluorenes derivatives bearing electron-donating aminostyryl substituents ($-\text{NH}_2$) at the 2,7- or 3,6-

positions, which exhibited the existence of a spiroconjugation effect and moderate to strong fluorescence emission [45]. Many studies show that silicon-containing π -conjugated compounds have recently been paid much attention due to their intense solid-state fluorescence and/or good electron transport properties in organic light-emitting diodes [46–52]. The siloles in particular have a relatively low-lying lowest unoccupied molecular orbital (LUMO) level owing to the $\sigma^*-\pi^*$ conjugation between the σ^* orbital of the exocyclic Si–C bond and the π^* orbital of the butadiene fragment. These unique electronic properties have led to very high electron affinity and, in some cases, nondispersing and air-stable electron transport [53, 54]. In this paper, our aim is to systematically investigate the second-order NLO properties and reorganization energy of silafluorenes and spirobisilafluorenes derivatives and build their relationship between their structures and properties. The effects of replacement of a silicon atom with carbon atom and replacement of $-\text{NH}_2$ with $-\text{NO}_2$ on NLO properties and reorganization energy are also investigated.

2 Computational details

Geometrical optimization of the twenty silafluorenes and spirobisilafluorenes derivatives without any symmetry constraint was carried out by employing B3LYP functional [55] in the density functional theory (DFT) level as implemented in Gaussian 03 program [56]. The geometrical structure and Cartesian coordinates are shown in Fig. S1 (supporting information). The B3LYP functional is a combination of Becke's three-parameter hybrid exchange functional [55] and the Lee–Yang–Parr [57] correlation functional. Basis sets of 6-31G* were applied to our studied systems. The single-excitation configuration interaction (CIS) method is adopted to obtain the first singlet excited-state (S1) structures, based on the ground state (S0) structures. Time-dependent density functional (TD-DFT) calculations were carried out at the B3LYP/6-31G* level to determine their absorption and emission energies and transition dipole moments. The second-order polarizabilities were calculated as performed in the Gaussian 03 program package. To evaluate electron correlation effects, the static second-order polarizability was also calculated at the second-order Møller-Plesset (MP2) level. The effects of six different basis sets (6-31G*, 6-311G*, 6-31 + G*, 6-311 + G*, 6-311 ++G*, 6-311 ++G**) on second-order polarizability are also discussed.

In general, electric-field-induced second harmonic generation (EFISHG) and hyper-Rayleigh scattering (HRS) are the two main methods to determine the second-order NLO properties. Here, we focused on the HRS response of the studied compounds. In the case of plane-polarized incident

light and observation made perpendicular to the propagation plane without polarization analysis of the scattered beam, the second-order NLO response that can be extracted from HRS data [58] can be described as:

$$\beta_{\text{HRS}}(-2\omega; \omega, \omega) = \sqrt{\{\langle \beta_{\text{ZZZ}}^2 \rangle + \langle \beta_{\text{XZZ}}^2 \rangle\}} \quad (1)$$

$\langle \beta_{\text{ZZZ}}^2 \rangle$ and $\langle \beta_{\text{XZZ}}^2 \rangle$ correspond to isotropic orientational averages of the β tensor components without assuming Kleinman's conditions [59] and are described as:

$$\begin{aligned} \langle \beta_{\text{ZZZ}}^2 \rangle &= \frac{1}{7} \sum_{\xi}^{x,y,z} \beta_{\xi\xi\xi}^2 + \frac{4}{35} \sum_{\xi}^{x,y,z} \beta_{\xi\xi\eta}^2 + \frac{2}{35} \sum_{\xi \neq \eta}^{x,y,z} \beta_{\xi\xi\xi} \beta_{\xi\eta\eta} \\ &+ \frac{4}{35} \sum_{\xi \neq \eta}^{x,y,z} \beta_{\eta\xi\xi} \beta_{\xi\xi\eta} + \frac{4}{35} \sum_{\xi \neq \eta}^{x,y,z} \beta_{\xi\xi\xi} \beta_{\eta\eta\xi} \\ &+ \frac{1}{35} \sum_{\xi \neq \eta}^{x,y,z} \beta_{\eta\xi\xi}^2 + \frac{4}{105} \sum_{\xi \neq \eta \neq \zeta}^{x,y,z} \beta_{\xi\xi\eta} \beta_{\eta\xi\xi} \\ &+ \frac{1}{105} \sum_{\xi \neq \eta \neq \zeta}^{x,y,z} \beta_{\eta\xi\xi} \beta_{\eta\xi\xi} + \frac{4}{105} \sum_{\xi \neq \eta \neq \zeta}^{x,y,z} \beta_{\xi\xi\eta} \beta_{\zeta\xi\eta} \end{aligned} \quad (2)$$

$$\begin{aligned} \langle \beta_{\text{XZZ}}^2 \rangle &= \frac{1}{35} \sum_{\xi}^{x,y,z} \beta_{\xi\xi\xi}^2 + \frac{4}{105} \sum_{\xi \neq \eta}^{x,y,z} \beta_{\xi\xi\xi} \beta_{\xi\eta\eta} - \frac{2}{35} \sum_{\xi \neq \eta}^{x,y,z} \beta_{\xi\xi\xi} \beta_{\eta\eta\xi} \\ &+ \frac{8}{105} \sum_{\xi \neq \eta}^{x,y,z} \beta_{\xi\xi\eta}^2 + \frac{3}{35} \sum_{\xi \neq \eta}^{x,y,z} \beta_{\xi\eta\eta}^2 - \frac{2}{35} \sum_{\xi \neq \eta}^{x,y,z} \beta_{\xi\xi\eta} \beta_{\eta\xi\xi} \\ &+ \frac{1}{35} \sum_{\xi \neq \eta \neq \zeta}^{x,y,z} \beta_{\xi\xi\eta} \beta_{\eta\xi\xi} - \frac{2}{105} \sum_{\xi \neq \eta \neq \zeta}^{x,y,z} \beta_{\xi\xi\xi} \beta_{\eta\eta\xi} \\ &- \frac{2}{105} \sum_{\xi \neq \eta \neq \zeta}^{x,y,z} \beta_{\xi\xi\eta} \beta_{\eta\xi\xi} + \frac{2}{35} \sum_{\xi \neq \eta \neq \zeta}^{x,y,z} \beta_{\xi\xi\xi}^2 \\ &- \frac{2}{105} \sum_{\xi \neq \eta \neq \zeta}^{x,y,z} \beta_{\xi\eta\xi} \beta_{\eta\xi\xi} \end{aligned} \quad (3)$$

The second-order polarizability values are consistent with convention B of Ref. [60]. All of the calculations in this work are carried out using the Gaussian 03 package.

3 Results and discussion

In this paper, twenty different silafluorenes and spirobisilafluorenes derivatives were investigated (Fig. S1). Before further discussion, it is necessary to explain the geometric characters and name meanings of these compounds. Each compound is labeled by four letters. For example, Si in **SiB2D** indicates that spiroatom is silicon, while the **B2** specifies that the number of branches is two and substituted positions are at the 3, 6-positions. In **SiB2'D**, the **B2'** means that the substituted positions are at the 3,7-positions and the number of branches is two. The letter **D** means that the

terminal substitution is the donor ($-\text{NH}_2$). To study the substituted effect of donor or acceptor (**D/A**), the letter **D** is changed into **A** meaning acceptor ($-\text{NO}_2$). To determine the better spiro-center between carbon and silicon, we replaced the silicon atom with carbon within all studied compounds.

3.1 Second-order polarizability

Many investigations have revealed that the optimized geometries at different levels or with different basis sets do not cause significant differences in the calculated NLO response values for most organic compounds [13, 61, 62]. However, the NLO polarizabilities are very sensitive to the basis sets especially to diffuse and polarization functions [9, 63, 64]. Here, six different basis sets (6-31G*, 6-311G*, 6-31 + G*, 6-311 + G*, 6-311 ++G*, 6-311 ++G**) were tested. To evaluate electron correlation effects, the static second-order polarizability was also calculated at the second-order Møller-Plesset (MP2) level with the six different basis sets. Firstly, the **SiB1D** was taken as an example to study the relationship between second-order polarizabilities and basis sets based on B3LYP and MP2 methods, respectively. The results are shown in Fig. 1. The values of the second-order polarizabilities become larger and larger from 6-31G* to 6-31 + G*. Then, the values of the second-order polarizabilities decrease slightly. But, the values of the second-order polarizabilities become converged from the 6-311 + G* basis set. However, Suponitsky et al. found that 6-31 + G* basis set is enough to their studied compounds [65]. The results obtained from the MP2 method are smaller than those of B3LYP method. However, the MP2 and B3LYP methods give consistent trends on the second-order polarizabilities, which is in accordance with the conclusion of the literature [66]. It should be noted that the systematic design of the improved materials for NLO applications primarily requires the knowledge of structure–property relations and the trends in NLO response rather than absolute values to provide systemic guidance to the experimentalists. To further study the relationship between the basis set and the number of the branch, the second-order polarizabilities of **SiB2D** were calculated at the six different basis sets by using B3LYP method. And the results are shown in Fig. S2 (supporting information). Again, the values of the second-order polarizabilities become converged to the 6-311 + G* basis set. Finally, the B3LYP/6-311 + G* was used in the following discussion.

Design of the molecules with high molecular NLO polarizabilities and appropriate optical transparency is an important step in the quest for effective NLO materials. The use of quantum chemical methods for the prediction of the molecular NLO properties is expected to provide some

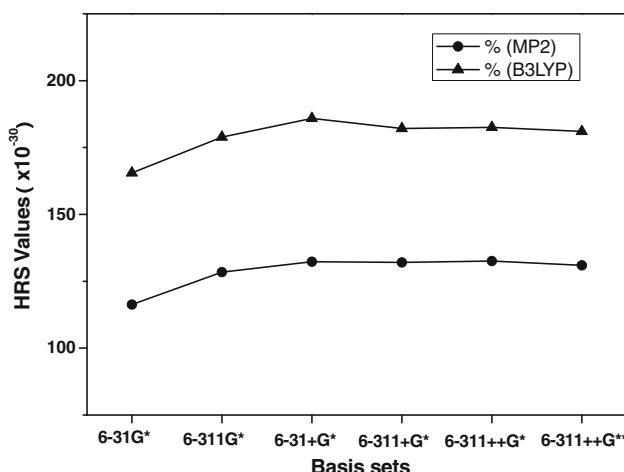


Fig. 1 The relationship between second-order polarizabilities and basis sets of system **SiB1D** obtained by MP2 and B3LYP method, respectively

instructions and accelerate subsequent experimental studies. The static second-order polarizability is termed the zero-frequency hyperpolarizability and is an estimate of the intrinsic molecular hyperpolarizability in the absence of resonance effect. The calculated second-order polarizability values of the studied compounds are given in Table 1. From Table 1, we can draw the following conclusions: (1) The second-order polarizability values increases with the increase in the number of branches, which means that increasing the number of branches can favor the charge transfer. (2) The second-order polarizability values of the compounds with the 3,6-positions substitution are great larger than those with the 2,7-positions substitution. (3) The second-order polarizability values of compounds containing the acceptor are greater and larger than those of compounds containing the donor. This indicates that compounds containing electronic acceptor matched with the direction of charge transfer. (4) To compounds containing the donor, the second-order polarizability values of compounds with the silicon atom as spiro-center are larger than those of compounds with the carbon atom as spiro-center. However, to compounds containing the acceptor, the second-order polarizability values of compounds with the silicon atom as spiro-center are smaller than those of carbon atom. This means there is certain cooperation between spiro-center and donor/acceptor.

3.2 Electronic spectra

3.2.1 Absorption spectra

To understand the structure–property relationship and optical transparency, the electronic excitation energies and oscillator strengths were calculated using the TDB3LYP at

Table 1 The calculated static second-order polarizabilities (10^{-30} esu) of the studied compounds at B3LYP/6-311 + G* level

Donor	β	Acceptor	β	Donor	β	Acceptor	β
SiB1D	182.13	SiB1A	335.69	CB1D	110.20	CB1A	372.66
SiB2D	259.04	SiB2A	374.28	CB2D	178.22	CB2A	428.87
SiB4D	351.57	SiB4A	335.37	CB4D	185.38	CB4A	556.26
SiB2'D	25.58	SiB2'A	22.29	CB2'D	33.61	CB2'A	159.92
SiB4'D	94.31	SiB4'A	108.82	CB4'D	8.07	CB4'A	102.68

6-31G* level (Table 2). From the complex SOS expression, the two-level model that linked between β_{CT} and a low-lying charge transfer transition has been established. For the static case, the following expression is employed to estimate β_{CT} :

$$\beta_{CT} \propto \frac{\Delta\mu f_{gm}}{E_{gm}^3} \quad (4)$$

where $\Delta\mu$ is the change of dipole moment between the ground and m th excited state, f_{gm} is the oscillator strength of the transition from the ground state (g) to the m th excited state (m), and E_{gm} is transition energy. Thus, the second-order polarizability caused by charge transfer (β_{CT}) is proportional to the optical intensity and inversely proportional to the cube of transition energy (E_{gm}). As a result, a larger f_{gm} with a lower E_{gm} will lead to the larger second-order polarizability. Our studied compounds have large energy gaps, and the model is valid for this analysis.

To be simple, the electronic transition properties of compounds with silicon as spiro-center were analysis due to the similarity of the compounds with carbon as spiro-center. The excitation energy decreases with the increase in the number of branches (Table 2). On the other hand, the number of states with larger oscillator strength increases with increase in the number of branches (Table 2). Those merits can increase the values of the second-order polarizability based on the two-level model. However, the NLO transparency can be maintained in the studied compounds, which is worthy of remarks in considering practical application. It should be noted that the excitation energies of compounds with acceptor is slightly smaller than those of compounds with donor. This can be used to explain why the compounds with acceptor have larger NLO response. However, the bathochromic shift extent of compounds with substituted positions at the 3,6-positions is slightly smaller than those with the substituted positions at the 2,7-positions, which is due to the difference in *p*-orbital delocalization between the 3,6- and 2,7-substituted biarylene ligands [67, 68].

To organic compounds, the electronic transition properties are mainly determined by the distribution of highest

Table 2 The calculated excitation energies (eV), oscillator strengths (*f*), main contribution of the studied compounds at the B3LYP/6-31G* level

Donor	Energy	<i>f</i>	Main contribution	Acceptor	Energy	<i>f</i>	Main contribution
SiB1D	367.82	0.6637	HOMO → LUMO	SiB1A	399.38	0.5466	HOMO → LUMO
SiB2D	387.84	0.4598	HOMO → LUMO	SiB2A	415.69	0.3761	HOMO → LUMO
	371.87	0.1886	HOMO-1 → LUMO		399.95	0.1173	HOMO-1 → LUMO
			HOMO → LUMO + 1				HOMO → LUMO + 1
SiB4D	408.01	0.2361	HOMO → LUMO	SiB4A	424.48	0.2561	HOMO → LUMO
	407.97	0.2386	HOMO → LUMO + 1		424.47	0.2560	HOMO → LUMO + 1
	390.75	0.2372	HOMO-1 → LUMO		405.36	0.6270	HOMO-2 → LUMO + 1
	390.71	0.2344	HOMO-1 → LUMO + 1				HOMO-3 → LUMO
	386.53	1.1458	HOMO-2 → LUMO + 1		398.55	0.1633	HOMO-1 → LUMO
			HOMO-3 → LUMO		398.54	0.1634	HOMO-1 → LUMO + 1
SiB2'D	436.51	2.0688	HOMO → LUMO	SiB2'A	468.20	2.0307	HOMO → LUMO
SiB4'D	453.49	0.0890	HOMO → LUMO	SiB4'A	468.55	0.3466	HOMO-1 → LUMO
			HOMO-1 → LUMO				HOMO → LUMO
	453.48	0.0891	HOMO → LUMO + 1		468.55	0.3469	HOMO → LUMO + 1
			HOMO-1 → LUMO + 1				HOMO-1 → LUMO + 1
	443.19	1.7615	HOMO → LUMO		458.20	1.6795	HOMO → LUMO
			HOMO-1 → LUMO				HOMO-1 → LUMO
	443.19	1.7617	HOMO → LUMO + 1		458.19	1.6799	HOMO → LUMO + 1
			HOMO-1 → LUMO + 1				HOMO-1 → LUMO + 1

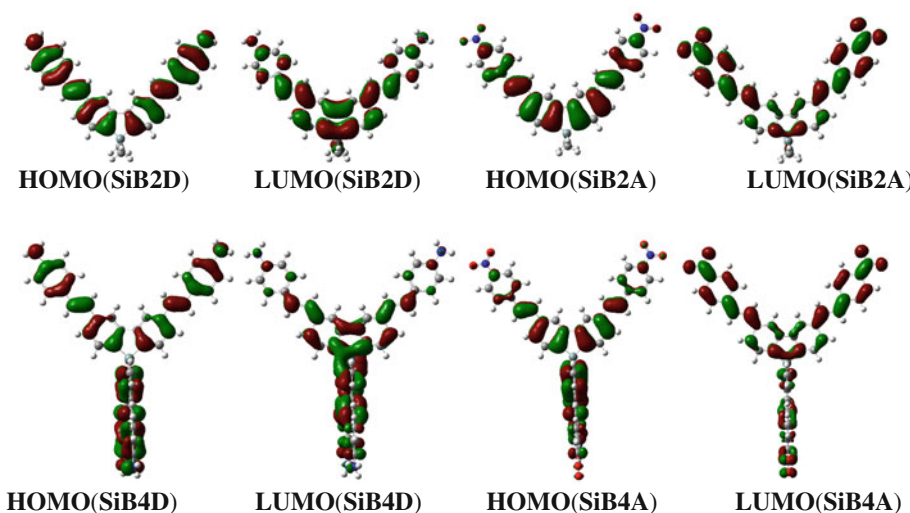
occupied molecular orbital (HOMO) and lowest unoccupied molecular orbital (LUMO). Here, compounds **SiB2D**, **SiB2A**, **SiB4D** and **SiB4A** are taken as examples to investigate the D/A substituted effects on charge transfer. And their frontier molecular orbitals are shown in Fig. 2. When comparing between compounds with the donor and acceptor, the distribution of HOMO and LUMO is different. When one electron was promoted from the HOMO to the LUMO (see Fig. 2), the orbital pattern in the donor-substituted compounds suggests that this electronic transition should be attributed to charge transfer from the peripheral phenyl groups to the central core and the silicon atoms also participate in this process. However, charge transfer of the acceptor substituted compounds is contrary.

3.2.2 Emission spectra

Based on the above discussion, the effects of different substitution positions and donor/acceptor substitution on second-order polarizabilities and electronic absorption spectra are obvious. To study these effects on the excited-state structures and emission spectra, the compounds with silicon as spiro-center were taken as examples due to the similarity of the compounds with carbon as spiro-center. The single-excitation configuration interaction (CIS) [69] method at 6-31G* level is adopted to obtain the first singlet excited-state (S_1) structures, based on the ground state (S_0) structures. Time-dependent density functional theory

(TDDFT) has emerged as the currently most applied method for molecular computations due to its balance between accuracy and efficiency. Then, the emission spectra are calculated at TDB3LYP/6-31G* level, and their results and experimental values are shown in Table S1. Our results indicate that the TDB3LYP maximum emission wavelengths are in good agreement with the experimental ones. From Table 1, we can find that the maximum emission wavelengths are red shift with increase in the number of branches. Compared with SiB1D, the bathochromic shift extent of compounds with the 3,6-positions substitution is smaller than that of compounds with the 2,7-positions substitution. It is interesting to note that oscillators' strengths of compounds with the 3,6-positions substitution are much smaller than that of compounds with the 2,7-positions substitution. The oscillators' strengths reflect the transition probability from the excited state to the ground state. In general, the higher the transition probability, the greater the emission probability and fluorescence kinetic constant can be obtained [70]. This means that compounds with the 2,7-positions substitution have the larger fluorescence quantum yields, which is also in agreement with the experimental results. The larger fluorescence quantum yields of these compounds are due to the result of expansion of π conjugation over the biarylene ligands [67, 68]. When comparing the donor/acceptor substitutions, the emission wavelengths with the acceptor substitution are larger than those of donor substitution, which can be

Fig. 2 The frontier molecular orbitals of the studied compounds SiB2D, SiB2A, SiB4D, and SiB4A



explained that the introduction of acceptor ($-\text{NO}_2$) decreases the LUMO energy level through π orbital interactions. Our results indicate that the maximum emission wavelengths and fluorescence quantum yields could be tuned by changing the substitution position and donor/acceptor.

3.3 Reorganization energy

The efficiency of OLEDs is determined by charge injection and transport, charge carrier balance, radiative decay of excitons, and light extraction. However, charge transport is one of the most important properties in the performance of OLEDs, OFETs, and organic solar cells. Thus, highly efficient OLEDs need both efficiency and balance of charge transport within the organic layer(s). Highly fluorescent or phosphorescent organic materials in OLEDs devices have either hole transport (*p*-type) or electron transport (*n*-type) characteristics. Currently, very often *p*-type behavior has been found to be dominating. Scarcity of *n*-type semiconductors influences the development of OLEDs in a certain extent [71]. Reorganization energy is usually used as the main aspect to assess the charge transport rate [72–76]. Moreover, the calculated reorganization energy in aromatic systems based on DFT theory is in good agreement with experimental results [77].

The electron (λ_e) and hole (λ_h) reorganization energies can be obtained by the following relationships:

$$\begin{aligned}\lambda_h &= [E^+(0) - E^+] + [E^0(+) - E^0(0)] \\ \lambda_e &= [E^0(-) - E^0(0)] + [E^-(0) - E^-(0)]\end{aligned}\quad (5)$$

where $E^+(0)$ is the energy of cationic stated in neutral geometry, $E^0(+)$ is the energy of neutral stated in cationic geometry, and the others are similar. The calculated reorganization energy of the studied compounds is shown in

Table 3 The calculated reorganization energy (eV) of the studied compounds at B3LYP/6-31G*

Donor	Hole	Electron	Acceptor	Hole	Electron
SiB1D	0.428	0.342	SiB1A	0.250	0.363
SiB2D	0.317	0.223	SiB2A	0.149	0.204
SiB4D	0.196	0.173	SiB4A	0.079	0.123
SiB2'D	0.371	0.280	SiB2'A	0.209	0.232
SiB4'D	0.210	0.158	SiB4'A	0.097	0.128
CB1D	0.417	0.337	CB1A	0.217	0.360
CB2D	0.294	0.196	CB2A	0.128	0.200
CB4D	0.169	0.115	CB4A	0.038	0.085
CB2'D	0.366	0.273	CB2'A	0.184	0.224
CB4'D	0.159	0.110	CB4'A	0.046	0.100

Table 3. Based on the analysis of these results, the following conclusions can be obtained: (1) The donor/acceptor (D/A) substitution has remarkable effect on the reorganization energy and can even change the transport properties as well as from the electronic transport material to the hole transport material. Specifically, to the compounds containing the donor ($-\text{NH}_2$), the electronic reorganization energy is smaller than that of hole reorganization energy. But, the electronic reorganization energy of compounds containing the acceptor ($-\text{NO}_2$) is larger than that of hole reorganization energy. Overall, the reorganization energy of compounds containing the acceptor ($-\text{NO}_2$) is smaller than that of compounds containing the donor ($-\text{NH}_2$), which means the acceptor substitution can greatly reduce the reorganization energy. (2) The reorganization energy greatly decreases with the increase in the number of branches, which means that increasing the number of branches can favor the charge transport. (3) The reorganization energy of compounds with substituted positions at the 3,6-positions is

smaller than those with the substituted positions at the 2,7-positions. This indicates that the 3,6-positions substitution is favor of the charge transport. There is a close relationship between charge transport and bond length modifications upon oxidation or reduction. In general, the smaller bond length modifications in these processes would exhibit the smaller reorganization energy, which would lead to the easier charge transport. According to the optimized structures of the neutral, anion, and cationic states, the average bond length modifications upon oxidation or reduction are compared among the studied compounds. The results show that the average bond length modifications greatly decrease with the increase in the number of branches. Moreover, the average bond length modifications of the compounds containing the acceptor ($-NO_2$) are smaller than those of compounds containing the donor ($-NH_2$). This means that the smaller reorganization energy results from the smaller bond length modifications. Tris(8-hydroxyquinolinato)aluminum(III) (**Alq**) is an excellent electronic transport material. The electronic reorganization energy of Alq is 0.276 eV. Our calculated electronic reorganization energy such as CB4'D (0.110 eV) is much smaller than that of Alq [9, 63, 64]. This makes them promising candidates for electronic transport material.

4 Conclusion

In this paper, we have investigated electronic absorption spectra, second-order polarizability and reorganization energy of the twenty silafluorenes and spirobisilafluorenes derivatives and elucidated structure–property relationships from the micromechanism. The basis sets and electron correlation effects are systematically investigated. The results show that the second-order polarizability (β) increases with increase in the number of the branches due to cooperative enhancement of the charge transfer, whereas the reorganization energy (λ) follows the opposite trend for the studied compounds. The properties (β and λ) of the compounds at the 3,6-positions substitution are much better than those of compounds at the 2,7-positions substitution. The charge transport properties can be tuned by changing the donor/acceptor (D/A) substitution and the acceptor substitution can greatly reduce the reorganization energy. The electronic absorption spectra show that all studied compounds can meet the requirement of nonlinear optical (NLO) transparency. Thus, increasing the number of branches and acceptor substitution can remarkably enhance performance of this kind of compounds. Based on larger β , smaller λ , and excellent optical transparency, this kind of compounds have a possibility to be excellent second-order NLO or charge transport materials.

Acknowledgments The authors gratefully acknowledge the financial support from the National Natural Science Foundation of China (Project No. 20903020), the Science and Technology Development Project Foundation of Jilin Province (20090146), the Training Fund of NENU's Scientific Innovation Project (NENU-STC08005), The Project Sponsored by the Scientific Research Foundation for the Returned Overseas Chinese Scholars, State Education Ministry, Science Foundation for Young Teachers of Jilin Agricultural University.

References

- Friend RH, Gymer RW, Holmes AB, Burroughes JH, Marks RN, Taliani C, Bradley DC, Dos Santos DA, Brédas JL, Lögdlund M, Salaneck WR (1999) *Nature* 397:121
- Skotheim TA, Elsenbaumer RL, Reynolds JR (eds) (1998) *Handbook of Conducting Polymers*. Marcel Dekker, New York
- Prasad PN, William DJ (1991) *Introduction to Nonlinear Optical Effects in Molecules and Polymer*. Wiley, New York
- Chemla DS, Zyss J (1987) *Nonlinear Optical Properties of Organic Molecules and Crystals*. Academic, New York
- Marder SR, Perry JW, Schaeffer WP (1989) *Science* 245:626
- Samuel IDW, Ledoux I, Dhenaut C, Zyss J, Fox HH, Schrock RR, Silbey RJ (1994) *Science* 265:1070
- Mukamel S, Wang HX (1992) *Phys Rev Lett* 69:65
- Spano FC, Soos ZG (1993) *J Chem Phys* 99:9265
- Kanis DR, Ratner MA, Marks TJ (1994) *Chem Rev* 94:195
- Marks TJ, Ratner MA (1995) *Angew Chem Int Ed Engl* 34:155
- Clays K, Persoons A (1991) *Phys Rev Lett* 66:2980
- Blau W (1987) *Phys Technol* 18:250
- Bredas JL, Adant C, Tackx P, Persoons A, Persoons BM (1994) *Chem Rev* 94:243
- Powell CE, Humphrey MG (2004) *Coord Chem Rev* 248:725
- Saragi TPI, Fuhrmann-Lieker T, Salbeck J (2006) *Adv Funct Mater* 16:966
- Tang CW, Van Slyke SA (1987) *Appl Phys Lett* 51:913
- Baldo MA, O'Brien DF, You Y, Shoustikov A, Sibley S, Thompson ME, Forrest SR (1998) *Nature* 395:151
- Garnier F, Hajlaoui R, Yassar A, Srivastava P (1994) *Science* 265:1684
- Sirringhaus H, Brown PJ, Friend RH, Nielsen MN, Bechgaard K, Langeveld-Voss BMW, Spiering AJH, Janssen RAJ, Meijer EW, Herwig P, de Leeuw DM (1999) *Nature* 401:685
- Sariciftci NS, Smilowitz L, Heeger AJ, Wudl F (1992) *Science* 258:1474
- Halls JMM, Walsh CA, Greenham NC, Marseglia EA, Friend RH, Moratti SC, Holmes AB (1995) *Nature* 376:498
- Hoffmann R, Imamura A, Zeiss GD (1967) *J Am Chem Soc* 89:5215
- Simmons HE, Fukunaga T (1967) *J Am Chem Soc* 89:5208
- Kim SY, Lee MY, Boo BH (1998) *J Chem Phys* 109:2593
- Abe J, Shirai Y, Nemoto N, Nagase Y (1997) *J Phys Chem A* 101:1
- Abe J, Shirai Y, Nemoto N, Nagase Y, Iyoda T (1997) *J Phys Chem B* 101:145
- Fu W, Feng JK, Pan GB (2001) *Theochem* 545:157
- Yang GC, Qin CS, Su ZM (2006) *J Phys Chem A* 110:4817
- Plaquet A, Guillaume M, Champagne B, Castet F, Ducasse L, Pozzo JL, Rodriguez V (2008) *Phys Chem Chem Phys* 10:6223
- Salbeck J (1996) In: Mauch RH, Gumlich HE (eds) *Proceedings of symposium on inorganic and organic electroluminescence (EL 1996)*, Wissenschaft und Technik, Berlin, Germany, p 243
- Bach U, Lupo D, Compte P, Moser JE, Weissertel F, Salbeck J, Spreitzer H, Grätzel M (1998) *Nature* 395:583

32. Salbeck J, Yu N, Bauer J, Weissörtel F, Bestgen H (1997) *Synth Met* 91:209
33. Steuber F, Staudigel J, Stössel M, Simmerer J, Winnacker A, Spreitzer H, Weissörtel F, Salbeck J (2000) *Adv Mater* 12:130
34. Huang J, Pfeiffer M, Blochwitz J, Werner A, Salbeck J, Liu S, Leo K (2001) *Jpn J Appl Phys* 40:6630
35. Tao YT, Ao L, Wang Q, Zhong C, Yang CL, Qin JG, Ma DG (2010) *Chem Asian J* 5:278
36. Saragi TPI, Pudzich R, Fuhrmann T, Salbeck J (2002) *Mater Res Soc Symp Proc* 725:89
37. Saragi TPI, Fuhrmann-Lieker T, Salbeck J (2005) *Synth Met* 148:267
38. Zhang XJ, Jiang XX, Luo J, Chi CY, Chen HZ, Wu JS (2010) *Chem Eur J* 16:464
39. Saragi TPI, Pudzich R, Fuhrmann T, Salbeck J (2004) *Appl Phys Lett* 84:2334
40. Heredia D, Natera J, Gervaldo M, Otero L, Fungo F, Lin CY, Wong KT (2010) *Org Lett* 12:12
41. Johansson N, Salbeck J, Bauer J, Weissörtel F, Bröms P, Andersson A, Salaneck WR (1999) *Synth Met* 101:405
42. Salbeck J, Schörner M, Fuhrmann T (2002) *Thin Solid Films* 417:20
43. Spehr T, Pudzich R, Fuhrmann T, Salbeck J (2003) *Org Electron* 4:61
44. Agou T, Hossain MD, Kawashima T, Kamada K, Ohta K (2009) *Chem Commun* 6762
45. Agou T, Hossain D, Kawashima T (2010) *Chem Eur J* 16:368
46. Tamao K, Uchida M, Izumizawa T, Furukawa K, Yamaguchi S (1996) *J Am Chem Soc* 118:11974
47. Yamaguchi S, Endo T, Uchida M, Izumizawa T, Furukawa K, Tamao K (2000) *Chem Eur J* 6:1683
48. Watkins NJ, Mäkinen AJ, Gao Y, Uchida M, Kafafi ZH (2004) *Proc Spie Int Soc Opt Eng* 5214:368
49. Palilis LC, Mäkinen AJ, Uchida M, Kafafi ZH (2003) *Appl Phys Lett* 82:2209
50. Palilis LC, Murata H, Uchida M, Kafafi ZH (2003) *Org Electron* 4:113
51. Uchida M, Izumizawa T, Nakano T, Yamaguchi S, Tamao K, Furukawa K (2001) *Chem Mater* 13:2680
52. Palilis LC, Uchida M, Kafafi ZH (2004) *IEEE J Sel Top Quantum Electron* 10:79
53. Murata H, Malliaras GG, Uchida M, Shen Y, Kafafi ZH (2001) *Chem Phys Lett* 339:161
54. Murata H, Kafafi ZH, Uchida M (2002) *Appl Phys Lett* 80:189
55. Becke AD (1993) *J Chem Phys* 98:5648
56. Frisch MJ, Trucks GW, Schlegel HB, Scuseria GE, Robb MA, Cheeseman JR, Montgomery JA Jr, Vreven T, Kudin KN, Burant JC, Millam JM, Iyengar SS, Tomasi J, Barone V, Mennucci B, Cossi M, Scalmani G, Rega N, Petersson GA, Nakatsuji H, Hada M, Ehara M, Toyota K, Fukuda R, Hasegawa J, Ishida M, Nakajima T, Honda Y, Kitao O, Nakai H, Klene M, Li X, Knox JE, Hratchian HP, Cross JB, Adamo C, Jaramillo J, Gomperts R, Stratmann RE, Yazyev O, Austin AJ, Cammi R, Pomelli C, Ochterski JW, Ayala PY, Morokuma K, Voth GA, Salvador P, Dannenberg JJ, Zakrzewski VG, Dapprich S, Daniels AD, Strain MC, Farkas O, Malick DK, Rabuck AD, Raghavachari K, Foresman JB, Ortiz JV, Cui Q, Baboul AG, Clifford S, Cioslowski J, Stefanov BB, Liu G, Liashenko A, Piskorz P, Komaromi I, Martin RL, Fox DJ, Keith T, Al-Laham MA, Peng CY, Nanayakkara A, Challacombe M, Gill PMW, Johnson B, Chen W, Wong MW, Gonzalez C, Pople JA (2003) *GAUSSIAN 03*, (Revision C.02). Gaussian Inc., Pittsburgh PA
57. Lee CT, Yang WT, Parr RG (1998) *Phys Rev B* 37:785
58. Mancois F, Sanguinet L, Pozzo JL, Guillaume M, Champagne B, Rodriguez V, Adamietz F, Ducasse L, Castet F (2007) *J Phys Chem B* 111:9795
59. Bersohn R, Pao YH, Frisch HL (1966) *J Chem Phys* 45:3184
60. Willetts A, Rice JE, Burland DA, Shelton DP (1992) *J Chem Phys* 97:7590
61. Yang ML, Li SH, Ma J, Jiang YS (2002) *Chem Phys Lett* 354:316
62. Sim F, Chin S, Dupuis M, Rice JE (1993) *J Phys Chem* 97:1158
63. Torrent-Sucarrat M, Sola M, Duran M, Luis JM, Kirtman B (2003) *J Chem Phys* 118:711
64. Skwara B, Bartkowiak W, Zawada A, Gora RW, Leszczynski J (2007) *Chem Phys Lett* 436:116
65. Suponitsky KY, Tafur S, Masunov AE (2008) *J Chem Phys* 129:044109
66. van Gisbergen SJA, Snijders JG, Baerends EJ (1998) *J Chem Phys* 109:10657
67. Dimitrakopoulos CD, Malenfant PRL (2002) *Adv Mater* 14:99
68. Babel A, Jenekhe SA (2003) *J Am Chem Soc* 125:13656
69. Foresman JB, Head-Gordon M, Pople JA, Frisch MJ (1992) *J Phys Chem* 96:135
70. Amati M, Lelj F (2002) *Chem Phys Lett* 358:144
71. Robey SW, Ciszek JW, Tour JM (2007) *J Phys Chem C* 111:17206
72. Malagoli M, Coropceanu V, da Silva Filho DA, Bredas JL (2004) *J Chem Phys* 120:7490
73. Coropceanu V, Malagoli M, da Silva Filho DA, Gruhn NE, Bill TG, Bredas JL (2002) *Phys Rev Lett* 89:275503
74. da Silva Filho DA, Friedlein R, Coropceanu V, Ohrwall G, Osikowicz W, Suess C, Sorensen SL, Svensson S, Salaneck WR, Bredas JL (2004) *Chem Commun* 1702
75. Gruhn NE, da Silva Filho DA, Bill TG, Malagoli M, Coropceanu V, Kahn A, Bredas JL (2002) *J Am Chem Soc* 124:7918
76. Coropceanu V, Kwon O, Wex B, Kaafarani BR, Gruhn NE, Durivage JC, Neckers DC, Bredas JL (2006) *Chem Eur J* 12:2073
77. Lin BC, Cheng CP, You ZQ, Hsu CP (2005) *J Am Chem Soc* 127:66